

## Pressure- and temperature-induced spin-state transition in single-crystalline $\text{La}_{1-x}\text{Sr}_x\text{CoO}_3$ ( $x=0.10$ and $0.33$ )

K. Mydeen,<sup>1</sup> P. Mandal,<sup>2</sup> D. Prabhakaran,<sup>3</sup> and C. Q. Jin<sup>1</sup><sup>1</sup>Beijing National Laboratory for Condensed Matter Physics, Institute of Physics, Chinese Academy of Sciences, Beijing 100 080, China<sup>2</sup>Saha Institute of Nuclear Physics, 1/AF Bidhannagar, Calcutta 700 064, India<sup>3</sup>Clarendon Laboratory, Department of Physics, University of Oxford, Oxford OX1 3PU, United Kingdom

(Received 19 February 2009; revised manuscript received 15 June 2009; published 21 July 2009)

We report on the temperature dependence of magnetization ( $M$ ) and resistivity ( $\rho$ ) of  $\text{La}_{1-x}\text{Sr}_x\text{CoO}_3$  ( $x=0.10$  and  $0.33$ ) single crystals. For  $x=0.10$ , the temperature dependence of field-cooled magnetization ( $M_{\text{FC}}$ ) and zero-field-cooled magnetization ( $M_{\text{ZFC}}$ ) are similar to that expected for a canonical spin-glass system. The thermal response of  $M_{\text{ZFC}}$  for  $x=0.33$  indicates a glassy ferromagnetic state. We observe that the ferromagnetic transition temperature  $T_C$  decreases and  $\rho$  increases rapidly with increasing pressure ( $P$ ) for the metallic sample ( $x=0.33$ ) while the dependence of  $\rho$  on  $P$  for the insulating sample ( $x=0.10$ ) is quite complicated; the pressure coefficient of resistivity ( $d\rho/dT$ ) is sensitive to temperature and applied pressure due to the strong interplay between the pressure-induced band broadening and spin-state transition phenomenon.  $d\rho/dT$  is large and negative at low-pressure and low-temperature regimes while small and positive at high pressures ( $P > 5.4$  GPa) and high temperatures ( $T > 110$  K).

DOI: [10.1103/PhysRevB.80.014421](https://doi.org/10.1103/PhysRevB.80.014421)

PACS number(s): 62.50.-p, 71.30.+h, 74.25.Fy, 75.50.Lk

### I. INTRODUCTION

Rare-earth cobaltates,  $R_{1-x}A_x\text{CoO}_3$  ( $R$ =rare-earth ion,  $A$  = Sr, Ba, and Ca), have received renewed attention due to the existence of temperature driven spin-state transition and unusual magnetic ground state. In undoped  $R\text{CoO}_3$ , trivalent Co ion is in a low-spin (LS) state ( $t_{2g}^6$ ,  $S=0$ ) due to the crystal-field splitting ( $\Delta_{CF}$ ) being slightly larger than the intra-atomic exchange energy  $J_{ex}$  (Hund's coupling). With increasing doping concentration ( $x$ ), the system exhibits a complicated magnetic phase diagram and becomes ferromagnetic above a critical value of  $x$ . Though the Co ions in  $R\text{CoO}_3$  are in LS configuration at low temperature, upon increasing temperature the system undergoes a spin-state transition at around 100 K. This phenomenon has been attributed to the thermal excitation of the LS state to either the intermediate-spin (IS) ( $t_{2g}^5e_g^1$ ,  $S=1$ ) or the high-spin (HS) ( $t_{2g}^4e_g^2$ ,  $S=2$ ) state.<sup>1-5</sup> The existence of such a spin-state transition indicates that the energy difference ( $\Delta$ ) between  $t_{2g}$  and  $e_g$  levels is rather small. As  $\Delta$  is small, there are several efforts to tune this energy scale through  $\Delta_{CF}$  and to study the effect of this change on electronic and magnetic properties.<sup>6-13</sup>  $\Delta_{CF}$  can be changed either by varying the sample composition (internal chemical pressure) or by applying external pressure ( $P$ ). The crystal symmetry, Co-O bond length, and Co-O-Co bond angle are sensitive to the size of the  $R$  ion. As  $R$  decreases the lattice symmetry changes from rhombohedral to orthorhombic and the Co-O-Co bond angle more and more deviates from  $180^\circ$ . Concomitantly, the crystal field  $\Delta_{CF}$  at the Co site slightly changes. Though the structural response to external pressure in cobaltates is, to some extent, similar to that observed in manganites and several other perovskites, the evolution of magnetic and transport properties with pressure is quite different. In manganites, both conductivity and ferromagnetic transition temperature ( $T_C$ ) increase with the increase in  $P$  due to the increase in bandwidth whereas in cobaltates the enhancement

of conductivity with  $P$  has hardly been observed. Indeed, the effect of pressure on these properties can be just opposite.<sup>8,9</sup> Lengsdorf *et al.*<sup>8</sup> studied the transport and magnetic properties of  $\text{La}_{0.82}\text{Sr}_{0.18}\text{CoO}_3$  single crystal and observed that conductivity, ferromagnetic moment, and  $T_C$  decrease with pressure. Similar behavior of magnetic properties has also been reported for  $\text{La}_{1-x}\text{Ca}_x\text{CoO}_3$ .<sup>9</sup> This unusual  $P$  dependence of transport and magnetic properties has been explained on the basis of spin-state transition from IS/HS to LS owing to the increase in  $\Delta_{CF}$  with increasing  $P$ .

In order to understand the intriguing origin of inhomogeneous magnetic ground state of cobaltates, we present, in this paper, the magnetic properties of both metallic ( $x=0.33$ ) and semiconducting ( $x=0.10$ ) single crystals of  $\text{La}_{1-x}\text{Sr}_x\text{CoO}_3$ . Our results demonstrate that the temperature and magnetic field ( $H$ ) dependence of magnetization ( $M$ ) of single crystals are quite different from that of polycrystalline samples. To elucidate the role of applied pressure on bandwidth and spin-state transition, we have studied the effect of high pressure on  $\rho$  of these samples. While for  $x=0.33$  sample, we observe a strong increase in  $\rho$ , in good agreement with the tendency to develop insulating state with increasing  $P$  reported for  $x=0.18$ ,<sup>8</sup> a more intricate pressure effect due to the strong interplay between pressure-induced bandwidth enhancement and spin-state transition is observed for  $x=0.10$  sample.

### II. EXPERIMENTAL DETAILS

Polycrystalline samples of nominal compositions  $\text{La}_{1-x}\text{Sr}_x\text{CoO}_3$  ( $0 \leq x \leq 0.33$ ) were synthesized by the conventional solid-state reaction technique using high-purity oxides and carbonates.  $\text{La}_2\text{O}_3$  was preheated at  $1100^\circ\text{C}$  for 12 h and  $\text{SrCO}_3$  was dried at  $150^\circ\text{C}$  for 6 h before weighting. The well-mixed powders were first calcined and then sintered in air at  $1000$ – $1100^\circ\text{C}$  for 5 days with intermediate grindings. The phase purity of the final product was checked by powder x-ray diffraction. Then the powders were pressed

into rods of size 12 mm diameter and 120 mm length with a hydraulic press. The rods were then sintered at 1200 °C for 6–12 h using a vertical sintering furnace. Single crystals of size 10 mm diameter and 10 cm length were grown from the polycrystalline rods by the traveling solvent float-zone method using a four-mirror image furnace (Crystal Systems Inc.). In order to achieve oxygen stoichiometry close to 3, Sr-doped crystals were grown in an oxygen atmosphere at a pressure of 5–9 bar. The typical growth rate was 3 mm/h. The phase purity and the crystalline quality were carefully checked by various techniques such as x-ray powder diffraction, Laue diffraction, and electron probe microanalysis. Both electron probe microanalysis and x-ray powder-diffraction data show that the crystals are pure and stoichiometrically correct. The sharp diffraction spots in neutron Laue pattern indicates the high crystalline quality of the samples and the whole crystal mosaic spread is about 1°. The powder-diffraction patterns of  $\text{La}_{1-x}\text{Sr}_x\text{CoO}_3$  can be indexed by a rhombohedral unit cell with the space group  $R\bar{3}c$ . The substitution of the larger  $\text{Sr}^{2+}$  at the site of  $\text{La}^{3+}$  progressively reduces the rhombohedral distortion present in the parent compound. The details structural analysis for different Sr concentration have been reported elsewhere.<sup>14</sup> The nature of the crystal surface was checked by optical and scanning electron microscopy (SEM). We observe that surface images of polished cross sections of the crystals obtained by SEM are smooth with no further evidence of microcracks or segregation. Thermogravimetric analysis (TGA) data were collected using a Rheometric Scientific STA1500 instrument to determine the oxygen content. Samples were loaded into alumina pans and heated under a flow (40 ml/min) of dilute hydrogen (10%) in nitrogen. We observe that the oxygen content in these samples is close to 3. The magnetic properties were studied using superconducting quantum interference device magnetometer (Quantum Design) and vibrating sample magnetometer (Oxford Instruments). The dc magnetization measurements were done along the direction of easy axis of  $M$  in the  $ac$  plane. Well-characterized single crystal was aligned with a goniometer using Laue diffraction and cut along the  $ac$  plane and the  $b$  axis. Then it was thinned and polished to a sheet of 30–50  $\mu\text{m}$  in thickness and cut into small pieces of  $\sim 100 \times 150 \mu\text{m}^2$  for the resistivity measurements. To achieve a wider pressure range with high resolution of resistivity data, we employed a diamond-anvil cell and embedded the conductive electrodes into the sample space for a four-probe electrical resistivity measurement along the  $ac$  plane. The sample and some small ruby chips were clamped in the sample space with FC-77 as a pressure transmitting medium. Determination of the pressure value was carried out by the ruby fluorescence method. The limitation of the facility restricts us to carry out the resistivity measurements under pressure down to 77 K only. The sharp magnetic transition and the absence of upturn in  $\rho$  at low temperature and the large residual resistivity ratio at ambient pressure (for  $x=0.33$ ) are the indications of good quality of the sample.

### III. RESULTS AND DISCUSSION

The temperature dependence of field-cooled (FC) magnetization ( $M_{\text{FC}}$ ) and zero-field-cooled (ZFC) magnetization

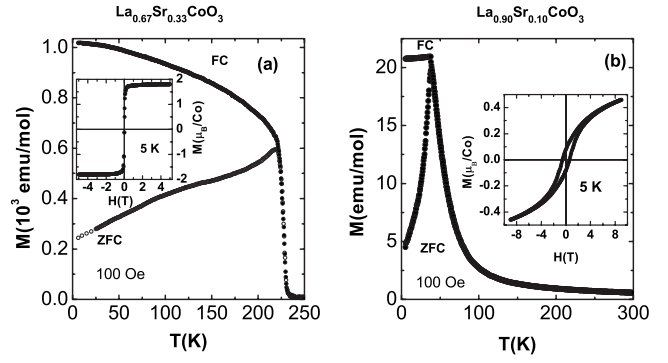


FIG. 1. (a) Temperature dependence of  $M_{\text{FC}}$  and  $M_{\text{ZFC}}$  for  $\text{La}_{0.67}\text{Sr}_{0.33}\text{CoO}_3$  single crystal measured at 100 Oe. Inset shows hysteresis loops of the magnetization at  $T=5$  K. (b) Temperature dependence of  $M_{\text{FC}}$  and  $M_{\text{ZFC}}$  for  $\text{La}_{0.9}\text{Sr}_{0.1}\text{CoO}_3$  single crystal measured at 100 Oe. Inset shows hysteresis loops of the magnetization at  $T=5$  K.

( $M_{\text{ZFC}}$ ) at 100 Oe for  $x=0.33$  and 0.10 samples are shown in Fig. 1. For  $x=0.33$ , both  $M_{\text{FC}}$  and  $M_{\text{ZFC}}$  increase sharply at  $T_c=228$  K. In the ferromagnetic state,  $M_{\text{FC}}$  increases slowly with decreasing temperature like a Brillouin function. In contrast,  $M_{\text{ZFC}}$  decreases with decreasing temperature below  $T_c$ . The appearance of a peak in  $M_{\text{ZFC}}$  is an important factor for understanding the nature of magnetic ground state of the cobaltates. This unusual behavior of  $M$  has been interpreted in terms of the ferromagnetic “cluster-glass” model.<sup>2,15,16</sup> According to this model, the system phase separates into hole-rich ferromagnetic clusters dominated by the ferromagnetic double-exchange interaction between heterovalent  $\text{Co}^{3+}$  and  $\text{Co}^{4+}$  ions, the clusters being embedded in a hole-poor matrix in which the magnetic interaction is dominated by the antiferromagnetic superexchange between isovalent  $\text{Co}^{3+}$  ions. In such a scenario, upon cooling in absence of magnetic field the hole-rich ferromagnetic clusters freeze into random orientations, dictated by the local anisotropy field. When field cooled the clusters align, leading to the onset of a large ferromagnetic-type magnetization. For further understanding the nature of the magnetic ground state, we have also investigated the field dependence of  $M$  for this sample [inset of Fig. 1(a)].  $M$  increases sharply with increasing field and a saturationlike behavior appears at fields above  $H \sim 2$  T. The value of spontaneous magnetization determined from the  $M(H)$  curve is  $\sim 1.8 \mu_B/\text{Co}$ . We observe that the hysteresis loop is very narrow and the values of both coercive field and remanent magnetization are quite small, as in the case of typical soft ferromagnets. A clear difference in the magnetic property of single crystal and polycrystalline samples is reflected in  $M(H)$  curve. Several earlier reports have also shown that the temperature and field dependence of the magnetization are quite different for single and polycrystalline samples.<sup>9,17,18</sup> Often,  $M$  of polycrystalline samples does not saturate but increases linearly with  $H$ .<sup>2,15,16,19</sup> The linear  $H$  dependence of  $M$  was explained on the basis of coexistence of two magnetic phases. According to this, the hysteresis loop of a ferromagnetic sample should not saturate rather increase linearly with  $H$  due to the presence of nonferromagnetic matrix of  $\text{Co}^{3+}$  spins with antiferromagnetic

interaction.<sup>15</sup> The absence of linear  $H$  dependence of  $M$  suggests that the amount of hole-poor matrix with antiferromagnetic interaction is very small in the present sample.

For the  $x=0.10$  sample, both  $M_{FC}$  and  $M_{ZFC}$  increase monotonically with decreasing  $T$  down to 38 K. Below 38 K,  $M_{FC}$  remains almost flat while  $M_{ZFC}$  decreases very rapidly and, as a result, it exhibits a huge cusp at  $T_{SG}=38$  K indicating the formation of a spin-glass state below  $T_{SG}$ . Above  $T_{SG}$ , no visible difference between ZFC and FC curves is observed. For  $x=0.10$  doping too, there are several important differences in the nature of  $T$  dependence of  $M_{ZFC}$  and  $M_{FC}$  of single crystal and those reported for polycrystalline samples. Unlike canonical spin-glass system, ZFC and FC curves start to bifurcate well above  $T_{SG}$  and a marked increase in  $M$  occurs below  $\sim 240$  K in polycrystalline samples for  $0.025 \leq x \leq 0.15$  compositions.<sup>2,15,19</sup> Below 240 K,  $M_{FC}$  is larger than  $M_{ZFC}$ . Different models such as microscopic phase separation and superparamagnetic clusters based on inhomogeneous magnetic state have been proposed to explain this behavior.<sup>2,15</sup> It was suggested that the increase in  $M$  at 240 K is due to the onset of magnetic order within the superparamagnetic cluster.<sup>2</sup> However, we did not observe any anomaly either in ZFC or in FC curve above  $T_{SG}$  associated with such ferromagnetic ordering. Our results are consistent with those expected for a canonical spin-glass system. We have also investigated the nature of  $H$  dependence of  $M$  for this sample up to 9 T [inset of Fig. 1(b)]. One can see that the  $H$  dependence of  $M$  of this sample is very different from that of the ferromagnetic metallic  $x=0.33$  sample.  $M$  increases with  $H$  without any sign of saturation up to the highest applied field. The small value and the lack of saturation in  $M$  at a relatively high field are the characteristics of a spin-glass system.

In order to elucidate the spin state of the Co ion at ambient pressure we have calculated the average spin ( $S$ ) of Co ions from the temperature dependence of paramagnetic susceptibility ( $\chi$ ) and the magnetic field dependence of  $M$  at low temperature well below  $T_C$ . In the paramagnetic phase,  $S$  can be extracted from the Curie-Weiss behavior of susceptibility,

$$\chi = \frac{C}{T - \theta}. \quad (1)$$

Here  $C$  [ $=N\mu_{eff}^2/3k$ ] is the Curie constant,  $\mu_{eff}=g[S(S+1)]^{1/2}\mu_B$  is the effective number of Bohr magnetons ( $\mu_B$ ),  $\theta$  is the paramagnetic Curie temperature,  $N$  is the number of Co ions per mol, and  $g$  is the Landé  $g$  factor. For both the samples, the inverse susceptibility  $\chi^{-1}$  ( $=H/M$ ) is plotted as a function of temperature up to 400 K in Fig. 2. It is clear from the figure that  $\chi$  does not obey the Curie-Weiss law over the whole range of temperature. For  $x=0.33$ ,  $\chi^{-1}(T)$  exhibits an upward curvature slightly above  $T_C$ . This behavior indicates the existence of critical fluctuations. On the other hand, for the  $x=0.10$  sample,  $\chi^{-1}(T)$  shows an approximate linear  $T$  dependence in the temperature range  $100 \text{ K} \leq T \leq 275 \text{ K}$  but a downward curvature appears at higher temperatures. The systematic enhancement of susceptibility at higher temperature is the indication of the occurrence of temperature-induced metal-

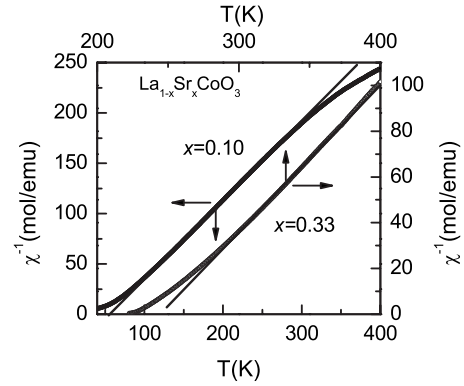


FIG. 2. Temperature dependence of inverse susceptibility ( $\chi^{-1}$ ) for  $\text{La}_{1-x}\text{Sr}_x\text{CoO}_3$  single crystals ( $x=0.10$  and  $0.33$ ) above the magnetic transitions. Solid lines are the Curie-Weiss linear fit to data.

insulator transition. From the linear  $T$  dependence of  $\chi^{-1}$ , we have determined  $\mu_{eff}$  and  $\theta$ . For  $x=0.10$ ,  $\mu_{eff}=3.2 \mu_B$  and  $\theta=55 \text{ K}$  whereas for  $x=0.33$  the corresponding values are  $3.44 \mu_B$  and  $245 \text{ K}$ , respectively. In these calculations we have used  $g=2$ . The estimated values of  $\mu_{eff}$  and  $\theta$  are comparable with those reported by different groups.<sup>2,11,15</sup> Based on the deduced values of  $\mu_{eff}$ , we can comment on the spin state of Co ion. The situation where  $\text{Co}^{3+}$  ions are in the IS state ( $S=1$ ) and the  $\text{Co}^{4+}$  ions are also in the IS state ( $S=3/2$ ) reveals spin-only moments  $\mu_{eff}=2.94$  and  $3.18 \mu_B$  for  $x=0.10$  and  $0.33$  compositions, respectively. Clearly our data are in better agreement with this configuration of the Co spin but differ significantly when other descriptions of  $\text{Co}^{4+}$  spin such as LS state ( $S=1/2$ ) or HS ( $S=5/2$ ) state are considered. From the magnetic susceptibility measurements in the paramagnetic state, it has been suggested that the IS state of Co ion is quite stable in  $\text{La}_{1-x}\text{Sr}_x\text{CoO}_3$  system over a wide range of doping ( $0.20 \leq x \leq 0.70$ ).<sup>15</sup> The spin state of Co ion can also be determined from the value of saturation moment  $M_S$  in the ferromagnetic phase. The saturation value of the magnetization in the ferromagnetic phase is  $1.8 \mu_B/\text{Co}$  for  $x=0.33$ . Though this ordered moment of  $\text{La}_{0.67}\text{Sr}_{0.33}\text{CoO}_3$  compound agrees quite well with the value reported from magnetization and neutron-diffraction experiments,<sup>16,20–22</sup> it is smaller than the expected spin-only moment ( $2.34 \mu_B$ ) when both  $\text{Co}^{3+}$  and  $\text{Co}^{4+}$  are in IS state. Indeed, the measured value of  $M_S$  is closer to the expected spin-only moment ( $1.67 \mu_B$ ) if  $\text{Co}^{3+}$  is in IS state but  $\text{Co}^{4+}$  is in LS state. So, the spin states of Co ions determined from the saturation moment and the paramagnetic susceptibility do not correspond to each other. Comparison of the value of  $M_S$  at 5 K with  $\mu_{eff}$  so calculated shows clearly that the number of unpaired spins is larger at higher temperatures. It has also been shown that  $M_S$  is very sensitive to the size of rare-earth ion.<sup>11</sup> For example, when La in  $\text{La}_{0.67}\text{Sr}_{0.33}\text{CoO}_3$  is replaced by Nd,  $M_S$  reduces to as low as  $0.37 \mu_B$ .<sup>11</sup> Thus it is difficult to determine the spin state of the Co ion from the saturation magnetization data as opposed to the high-temperature Curie-Weiss behavior. This behavior is quite different from that observed in manganites where the measured  $M_S$  is consistent with the ionic picture and almost insensitive to rare-earth ion. Such difference between manganites and cobal-

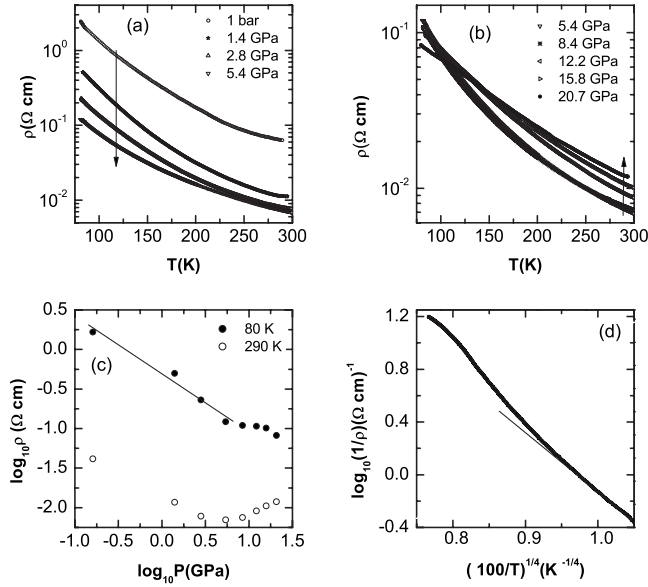


FIG. 3. (a) Temperature dependence of the resistivity ( $\rho$ ) up to 5.4 GPa for  $\text{La}_{0.9}\text{Sr}_{0.1}\text{CoO}_3$  single crystal. The arrow indicates the direction of increase in  $P$ . (b) Temperature dependence of  $\rho$  up to 20.7 GPa for  $\text{La}_{0.9}\text{Sr}_{0.1}\text{CoO}_3$  single crystal. The arrow indicates the direction of increase in  $P$ . (c) The log-log plots of  $P$  dependence of  $\rho$  for  $\text{La}_{0.9}\text{Sr}_{0.1}\text{CoO}_3$  single crystal at 80 and 290 K. The solid line is the guide to the eyes for  $P < 8.4$  GPa. (d)  $\log_{10}(1/\rho)$  versus  $(100/T)^{1/4}$  plot for  $\text{La}_{0.9}\text{Sr}_{0.1}\text{CoO}_3$  single crystal at ambient pressure. The solid line shows the slope of the curve at around 80 K.

tates may be related to the nature of magnetism in these two systems. In manganites, the conduction electrons are almost fully spin polarized due to the strong Hund's coupling, i.e., one expects spin-only moment of Mn ion. On the other hand, the higher conductivity in the ferromagnetic phase as well as in the paramagnetic phase, the lack of discontinuities in the transport properties at  $T_C$  and the absence of colossal magnetoresistance effect are the indications of bandlike ferromagnetism in cobaltates.<sup>11</sup> From the spin-density-functional calculations, Ravindran *et al.*<sup>23</sup> have shown that hole doping in this material reduces ionic character, enhancing hybridization between cobalt and oxygen ions, and uniformly affects the spin state of both  $\text{Co}^{3+}$  and  $\text{Co}^{4+}$  ions. Due to this Co-O hybridization, the expected average Co moment is reduced significantly compared to the simple ionic model prediction. They have also deduced the energetics of different spin configurations and observed that hole doping in  $\text{La}_{1-x}\text{Sr}_x\text{CoO}_3$  stabilizes the IS state of the Co ion.

Figures 3(a) and 3(b) show the temperature dependence of resistivity ( $\rho$ ) for some selected applied pressures up to 20.7 GPa for  $x=0.10$  sample. The  $\rho(T)$  curve at ambient pressure shows a semiconductinglike behavior and exhibits no evidence of ferromagnetic cluster state. As is apparent from Fig. 3, with increasing pressure up to  $P_c=5.4$  GPa,  $\rho$  at 80 K decreases dramatically, indicating a strong enhancement of electron hopping.  $\rho$  decreases considerably at room temperature also. By increasing the pressure above 5.4 GPa, however, we observe that  $P$  dependence of  $\rho$  is no longer simple but sensitive to the temperature regions. At low temperatures  $T < 110$  K,  $\rho$  decreases very slowly with  $P$  up to 20.7 GPa

whereas at high temperatures  $\rho$  increases with increasing  $P$  above 5.4 GPa. This indicates the presence of two competing interactions—one is dominating in the low-pressure region whereas other is dominating at high-pressure side. For quantitative understanding the role of these two competitive interactions, we have plotted the values  $\rho$  at 80 and 290 K as a function of  $P$  [Fig. 3(c)]. Figure 3(c) clearly demonstrates two distinct pressure regions depending on the effect of  $P$  on  $\rho$ . The resistivity at 80 K shows a power law decrease at low pressures. The decrease in  $\rho$  with increasing  $P$  at low temperature is consistent with the results reported for the manganites and other transition-metal oxides.<sup>8</sup> This can be explained on the basis of bandwidth broadening with increasing  $P$ . It has been shown that the Co-O bond length in  $\text{LaCoO}_3$  decreases with increasing pressure up to 8 GPa.<sup>7</sup> On the other hand, the Co-O-Co bond angle shows a nonmonotonic dependence on  $P$ . Initially the bond angle increases rapidly with increasing  $P$  up to about 4 GPa and then decreases slowly with further increase in  $P$ . Though, Co-O bond length decreases above 4 GPa, the rate of decrease is smaller by a factor of 4. This indicates that there is a critical value of  $P$ , which clearly separates two different regions of  $P$  dependence of structural properties. The decrease in the bond length and the increase in the bond angle with increasing pressure are common features in several perovskites and similar systems, and are known to enhance the electron hopping, thereby stabilizing the metallic state.<sup>8</sup>

Above 5.4 GPa, the resistivity of the system shows a very weak response over the entire temperature range. Though  $\rho$  decreases with increasing  $P$  at low temperatures, the rate of decrease is very small. On the other hand, the pressure coefficient of  $\rho$  is positive at high temperatures. The increase in  $\rho$  can also be explained on the basis of pressure dependence of structural parameters. We have already discussed that the Co-O-Co bond angle in  $\text{LaCoO}_3$  decreases slowly with increasing  $P$  above 4 GPa. Such a decrease in Co-O-Co bond angle at high pressures may suppress the charge-transfer process considerably and lead to resistivity increase. An alternative explanation for the increase in  $\rho$  with  $P$  is the pressure-induced spin-state transition of  $\text{Co}^{3+}$  ion from the magnetic IS/HS state to a nonmagnetic LS state. As the spin-state transition for the insulating samples is more effective at high temperatures, the low-temperature conduction is dominated by the weak hopping of electrons between the LS states of  $t_{2g}$  level, i.e., from  $(t_{2g}^6, S=0)$  state of  $\text{Co}^{3+}$  to  $(t_{2g}^5, S=1/2)$  of  $\text{Co}^{4+}$  for the present  $x=0.10$  sample. However, a significant amount of  $\text{Co}^{3+}$  undergoes a transition to the IS/HS state with increasing temperature and, as a consequence, the charge transfer between  $e_g$  levels, i.e., from  $(t_{2g}^5 e_g^1, S=1)$  state of  $\text{Co}^{3+}$  to  $(t_{2g}^5 e_g^0, S=1/2)$  state of  $\text{Co}^{4+}$  is enhanced. This suggests that at ambient pressure the resistivity at high temperatures is dominated by the spin-state transition phenomenon. In support of this argument, we have plotted  $\log_{10}(1/\rho)$  at ambient pressure as a function of  $T^{-1/4}$  in Fig. 3(d).<sup>24</sup> It is clear from the figure that in the high-temperature regime conductivity ( $1/\rho$ ) increases with increasing  $T$  at a faster rate than in the low-temperature regime. This behavior is consistent with the spin-state transition. The systematic enhancement of  $\chi^{-1}$  at low temperatures below 80 K (in Fig. 2) also supports the spin-state transition in this material. It has been

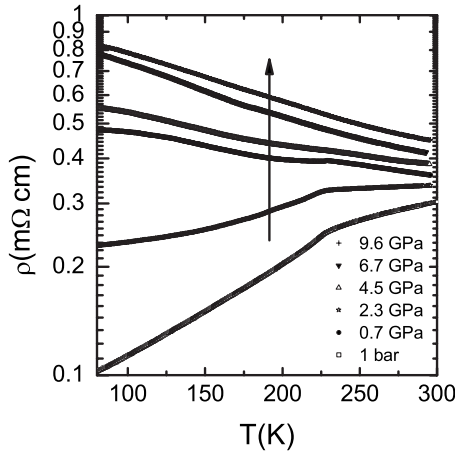


FIG. 4. Temperature dependence of  $\rho$  at different pressures up to 9.6 GPa for  $\text{La}_{0.67}\text{Sr}_{0.33}\text{CoO}_3$  single crystal. The arrow indicates the direction of increase in  $P$ .

observed that the crystal-field splitting in  $\text{La}_{1-x}\text{Sr}_x\text{CoO}_3$  increases remarkably with increasing pressure.<sup>7,8,25</sup> Thus, pressure is expected to favor the population of the LS state at the cost of depopulation of the IS/HS state. A direct consequence of such a pressure-induced transition from the magnetic IS/HS to a nonmagnetic LS state would be a net reduction in the saturation moment of Co. This will lead to resistivity enhancement. However, the contribution from the spin-state transition on magnetic and transport properties will be dominant as long as the crystal field is small, i.e., in the low-pressure regime. At high pressures above 5.4 GPa, the crystal field is already large and thus the contribution from the pressure-induced IS/HS to LS transition is expected to be very weak. In other words, at high pressures, the spin-state degree of freedom is not an important parameter to control the charge-transfer process. Combining the reported structural data<sup>7</sup> and the present resistivity results, we can say that the applied pressure has dual role on the conductivity. At low  $P$  where Co-O bond length decreases and Co-O-Co bond angle increases faster with increasing  $P$ , conductivity increases mainly due to the increase in bandwidth with pressure. On the other hand, the decrease in conductivity at high-temperature and high-pressure regimes is mainly due to the decrease in Co-O-Co bond angle with increasing  $P$ .

Figure 4 shows  $T$  dependence of  $\rho$  at different pressures up to  $P=9.6$  GPa for the  $x=0.33$  sample. At ambient pressure, the  $T$  dependence of  $\rho$  shows metallic behavior ( $d\rho/dT > 0$ ) in the paramagnetic as well as in the ferromagnetic regions. The ferromagnetic transition is indicated by a sharp drop in resistivity with lowering temperature. The weak anomaly at  $T_C$  with an increase in the slope  $d\rho/dT$  on decreasing temperature is probably due to the freezing out of spin disorder scattering. One can see that the  $P$  dependence of  $\rho$  of this sample is very different from that of the semiconducting  $x=0.10$  sample. The electrical resistivity increases with increasing  $P$  up to 9.6 GPa over the entire range of  $T$ , indicating a strong suppression of electron hopping with increasing  $P$ . Though,  $T_C$  decreases very slowly with increasing  $P$  at lower pressure, it is difficult to monitor the change in  $T_C$  due to the smearing out of the ferromagnetic

transition and the change in the nature of  $\rho(T)$  curve to semi-conductinglike at higher pressure. The monotonous increase in  $\rho$  and the decrease in  $T_C$  with the increase in  $P$  suggest that in the metallic sample the effect of broadening of bandwidth on  $\rho$  is much weaker as compared to that of spin-state transition. This is not quite unexpected and can be explained. The small value of  $\rho$  and the positive  $d\rho/dT$  suggest that the bandwidth of this sample is large. As the bandwidth is already large, application of external pressure may not influence bandwidth significantly. Lengsdorf *et al.*<sup>8</sup> studied the effect of  $P$  on  $\rho$  and  $M$  on a barely metallic sample with  $x=0.18$ , which is located in the close vicinity of metal-insulator transition. They observed that conductivity, ferromagnetic moment, and  $T_C$  decrease rapidly with pressure up to 5.7 GPa due to the spin-state transition but  $\rho$  decreases slowly with  $P$  above 5.7 GPa due to the increase in bandwidth. This means that the spin-state transition dominates conductivity in the low-pressure regime whereas the pressure-induced bandwidth increase dominates conductivity at high pressures. Though  $\rho$  increases with  $P$  for both  $x=0.18$  and 0.33 samples, there is a huge difference in the magnitude of the pressure-induced change in the resistivity between the two concentrations. For the present  $x=0.33$  sample, we observe at about 6 GPa an increase in a factor of 1.3 and less than 1 order of magnitude at 300 and 80 K, respectively. In contrast,  $\rho$  increases by more than 2 orders and 4 orders of magnitude at 300 and 80 K, respectively for  $x=0.18$ .<sup>8</sup> This difference is mainly related to a pressure-induced competition between antiferromagnetic superexchange and ferromagnetic double-exchange interactions near and well above the percolation concentration for the insulator-metal transition ( $x_{MI}=0.2$ ) and may be understood from the nature of evolution of electronic and magnetic properties of the system with doping concentration  $x$ . Both  $\text{La}_{1-x}\text{Sr}_x\text{CoO}_3$  and  $\text{La}_{1-x}\text{Ba}_x\text{CoO}_3$  show a few orders of magnitude change in  $\rho$  with a small variation in  $x$  at the percolation concentration.<sup>15,17</sup> As superexchange and double-exchange interactions are of comparable strength for  $x$  close to  $x_{MI}$ , a small increase or decrease in superexchange interaction either due to the applied pressure or doping may cause a huge change in  $\rho$ .<sup>8,15,17</sup> At higher doping level well above  $x_{MI}$  where the ferromagnetic interaction is much stronger than the superexchange resistivity is expected to change slowly with doping and pressure.

#### IV. CONCLUSION

In conclusion, we have investigated transport and magnetic properties of high-quality single crystals of  $\text{La}_{1-x}\text{Sr}_x\text{CoO}_3$ . For  $x=0.10$ ,  $M_{ZFC}(T)$  displays a huge cusp at  $T_{SG}=38$  K whereas  $M_{FC}(T)$  becomes almost  $T$  independent below  $T_{SG}$  as expected for a canonical spin-glass system.  $M_{FC}$  and  $M_{ZFC}$  neither bifurcate nor do show any anomalous increase above  $T_{SG}$ . The field dependence of magnetization for  $x=0.33$  is similar to that of a typical ferromagnet. The effect of pressure on resistivity of these samples is quite unusual due to the strong interplay between pressure-induced band broadening and pressure- and temperature-induced

spin-state transition from IS/HS to LS of  $\text{Co}^{3+}$ . For  $x=0.10$ ,  $\rho$  decreases with the increase in  $P$  up to 5.4 GPa due to the increase in bandwidth. Above 5.4 GPa,  $\rho$  at high temperatures increases with  $P$  mainly due to the decrease in Co-

O-Co bond angle. For  $x=0.33$ , pressure-induced spin-state transition dominates the charge transport over the entire range of pressure and, as a result,  $\rho$  increases with the increase in  $P$ .

- 
- <sup>1</sup>P. M. Raccah and J. B. Goodenough, *Phys. Rev.* **155**, 932 (1967).
- <sup>2</sup>M. A. Señaris-Rodríguez and J. B. Goodenough, *J. Solid State Chem.* **116**, 224 (1995); **118**, 323 (1995).
- <sup>3</sup>K. Asai, O. Yokokura, N. Nishimori, H. Chou, J. M. Tranquada, G. Shirane, S. Higuchi, Y. Okajima, and K. Kohn, *Phys. Rev. B* **50**, 3025 (1994).
- <sup>4</sup>S. Yamaguchi, Y. Okimoto, and Y. Tokura, *Phys. Rev. B* **55**, R8666 (1997).
- <sup>5</sup>M. W. Haverkort, Z. Hu, J. C. Cezar, T. Burnus, H. Hartmann, M. Reuther, C. Zobel, T. Lorenz, A. Tanaka, N. B. Brookes, H. H. Hsieh, H.-J. Lin, C. T. Chen, and L. H. Tjeng, *Phys. Rev. Lett.* **97**, 176405 (2006).
- <sup>6</sup>R. Lengsdorf, J.-P. Rueff, G. Vankó, T. Lorenz, L. H. Tjeng, and M. M. Abd-Elmeguid, *Phys. Rev. B* **75**, 180401(R) (2007).
- <sup>7</sup>T. Vogt, J. A. Hriljac, N. C. Hyatt, and P. Woodward, *Phys. Rev. B* **67**, 140401(R) (2003).
- <sup>8</sup>R. Lengsdorf, M. Ait-Tahar, S. S. Saxena, M. Ellerby, D. I. Khomskii, H. Micklitz, T. Lorenz, and M. M. Abd-Elmeguid, *Phys. Rev. B* **69**, 140403(R) (2004), and references therein.
- <sup>9</sup>I. Fita, R. Szymczak, R. Puzniak, I. O. Troyanchuk, J. Fink-Finowicki, Ya. M. Mukovskii, V. N. Varyukhin, and H. Szymczak, *Phys. Rev. B* **71**, 214404 (2005).
- <sup>10</sup>D. P. Kozlenko, N. O. Golosova, Z. Jiráček, L. S. Dubrovinsky, B. N. Savenko, M. G. Tucker, Y. Le Godec, and V. P. Glazkov, *Phys. Rev. B* **75**, 064422 (2007).
- <sup>11</sup>M. Paraskevopoulos, J. Hemberger, A. Krimmel, and A. Loidl, *Phys. Rev. B* **63**, 224416 (2001).
- <sup>12</sup>H. Masuda, T. Fujita, T. Miyashita, M. Soda, Y. Yasui, Y. Kobayashi, and M. Sato, *J. Phys. Soc. Jpn.* **72**, 873 (2003).
- <sup>13</sup>J. Baier, S. Jodlauk, M. Kriener, A. Reichl, C. Zobel, H. Kierspel, A. Freimuth, and T. Lorenz, *Phys. Rev. B* **71**, 014443 (2005).
- <sup>14</sup>D. Prabhakaran, A. T. Boothroyd, F. R. Wondre, and T. J. Prior, *J. Cryst. Growth* **275**, e827 (2005).
- <sup>15</sup>J. Wu and C. Leighton, *Phys. Rev. B* **67**, 174408 (2003), and references therein.
- <sup>16</sup>M. Itoh, I. Natori, S. Kubota, and K. Motoya, *J. Magn. Magn. Mater.* **140-144**, 1811 (1995); *J. Phys. Soc. Jpn.* **63**, 1486 (1994).
- <sup>17</sup>M. Kriener, C. Zobel, A. Reichl, J. Baier, M. Cwik, K. Berggold, H. Kierspel, O. Zabara, A. Freimuth, and T. Lorenz, *Phys. Rev. B* **69**, 094417 (2004).
- <sup>18</sup>H. M. Aarbogh, J. Wu, L. Wang, H. Zheng, J. F. Mitchell, and C. Leighton, *Phys. Rev. B* **74**, 134408 (2006).
- <sup>19</sup>P. Mandal, A. Hassen, and P. Choudhury, *J. Appl. Phys.* **100**, 103912 (2006); P. Mandal, P. Choudhury, S. K. Biswas, and B. Ghosh, *Phys. Rev. B* **70**, 104407 (2004).
- <sup>20</sup>M. Itoh and J. Natori, *J. Phys. Soc. Jpn.* **64**, 970 (1995).
- <sup>21</sup>V. G. Sathe, A. V. Pimpale, V. Siruguri, and S. K. Paranjpe, *J. Phys.: Condens. Matter* **8**, 3889 (1996).
- <sup>22</sup>R. Caciuffo, D. Rinaldi, G. Barucca, J. Mira, J. Rivas, M. A. Senaris-Rodríguez, P. G. Radaelli, D. Fiorani, and J. B. Goodenough, *Phys. Rev. B* **59**, 1068 (1999).
- <sup>23</sup>P. Ravindran, H. Fjellvag, A. Kjekshus, P. Blaha, K. Schwarz, and J. Luitz, *J. Appl. Phys.* **91**, 291 (2002).
- <sup>24</sup>Though  $\log_{10}(1/\rho)$  versus  $T^{-1/4}$  curve shows a weaker upward curvature as compared to  $\log_{10}(1/\rho)$  versus  $1/T$  curve, we also observe a faster increase in conductivity with increasing  $T$  in the high-temperature regime in the latter plot.
- <sup>25</sup>K. Asai, O. Yokokura, M. Suzuki, T. Naka, T. Matsumoto, H. Takahashi, N. Mōri, and K. Kohn, *J. Phys. Soc. Jpn.* **66**, 967 (1997).